Reduced Trap State Density in AlGaN/GaN HEMTs with Low-Temperature CVD-Grown BN Gate Dielectric

Ziyi He[1,b], Xiang Zhang[2,b], Tymofii S. Pieshkov[2,6], Ali Ebadi Yekta[3], Tanguy Terlier[5], Dinusha Herath Mudiyanselage[1], Dawei Wang[1], Bingcheng Da[1], Mingfei Xu[4], Shisong Luo[4], Cheng Chang[4], Tao Li[4], Robert J. Nemanich[3], Yuji Zhao[4,a], Pulickel M. Ajayan[2,a], Houqiang Fu[1,a]

AFFILIATIONS

[1]School of Electrical, Computer, and Energy Engineering, Arizona State University, Tempe, Arizona 85282, USA

[2]Department of Materials Science and Nanoengineering, Rice University, Houston, TX, 77005, USA

[3]Department of Physics, Arizona State University, Tempe, Arizona 85282, USA

[4]Department of Electrical and Computer Engineering, Rice University, Houston, TX, 77005, USA

[5]SIMS laboratory, Shared Equipment Authority, Rice University, 6100 Main Street, 77005 Houston Texas, United States.

[6]Applied Physics Graduate Program, Smalley-Curl Institute, Rice University, Houston, TX, 77005, USA

[a)]Authors to whom correspondence should be addressed: yuji.zhao@rice.edu, ajayan@rice.edu, houqiang@asu.edu.

[b)] These authors contributed equally to this work

Keywords

Boron nitride, Microwave-plasma-assisted chemical vapor deposition, Low-temperature growth, AlGaN/GaN high electron mobility transistors, trap state density.

ABSTRACT

In this letter, low-temperature (400 °C) chemical vapor deposition (CVD)-grown boron nitride (BN) was investigated as the gate dielectric for AlGaN/GaN metal-insulator-semiconductor high electron mobility transistors (MIS-HEMTs) on Si substrate. Comprehensive characterizations using X-ray photoelectron spectroscopy (XPS), reflection electron energy loss spectroscopy (REELS), atomic force microscope (AFM), high-resolution transmission electron microscopy (HRTEM), and time-of-flight secondary ion mass spectrometry (ToF-SIMS) were conducted to analyze the deposited BN dielectric. Compared with conventional Schottky-gate HEMTs, the MISHEMTs exhibited significantly enhanced performance with three orders of magnitude lower reverse gate leakage current, a lower off-state current of 1×10^{-7} mA/mm, a higher on/off current ratio of 10^8, and lower on-resistance of 5.40 Ω·mm. The frequency-dependent conductance measurement was performed to analyze the BN/HEMT interface, unveiling a low interface trap state density (D_{it}) on the order of 5×10^{11}-6×10^{11} $cm^{-2}\cdot eV^{-1}$. This work shows the effectiveness of low-temperature BN dielectrics and their potential for advancing GaN MISHEMTs toward high-performance power and RF electronics applications.

AlGaN/GaN high electron mobility transistors (HEMTs) are considered next-generation devices for high-power and high-frequency applications due to the large bandgap and high critical electric field of GaN and high-mobility two-dimensional electron gas (2DEG) at the AlGaN/GaN interface.[1-3] Nevertheless, the performance of conventional Schottky-gate AlGaN/GaN HEMTs has been limited by high gate leakage currents. Metal–insulator–semiconductor AlGaN/GaN HEMTs (MISHEMTs) with gate dielectrics have been proposed as an effective solution to suppress the leakage current of conventional Schottky-gate HEMTs and improve device performance.[1-3,14,15] Trap states at the dielectric/III-nitride interface and inside the dielectric play a critical role in GaN HEMTs, and the dynamic charging/discharging processes of these traps could lead to threshold voltage instability.[1,3,15] Therefore, selecting a suitable dielectric and improving the interface quality between the dielectric and GaN is of great importance.

Boron nitride (BN) possesses an ultrawide bandgap of ~6 eV, excellent chemical inertness, high thermal conductivity, and robust mechanical strength, which emerges as a promising dielectric material for power electronic devices.[4,6,7] Particularly, for GaN-based devices, BN eliminates Ga-O-related interface traps present in oxide-based dielectrics. Various synthesis methods for BN have been demonstrated, such as chemical vapor deposition (CVD), physical vapor deposition (PVD), mechanical exfoliation, and liquid exfoliation.[8-11,15,16] Among these methods, CVD techniques have the advantage of scalable growth of BN films. The direct growth of BN on GaN avoids the additional transfer process, reducing the time and potential contaminations during the transfer. However, the CVD synthesis temperature of BN typically exceeds 1000 °C.[10,11] Such a high temperature could lead to the degradation of GaN surface and increase the surface defects. While the commonly used gate dielectric SiN_x, SiO_2 and Al_2O_3 deposited by PECVD or atomic layer deposition (ALD) at relatively low temperature (e.g., 300 °C–400 °C) helps maintain GaN surface morphology, these growth methods also lead to high defects density in the dielectrics, causing the reliability issue of the device.[1,3] In this study, we successfully grew high-quality BN gate dielectric on AlGaN/GaN MISHEMT using low-temperature (400 °C) CVD with microwave plasma. The BN/AlGaN/GaN MISHEMT exhibited improved output current density (I_{dmax}) and three orders of magnitude lower reverse gate leakage current in comparison to conventional Schottky-gate HEMTs. This work opens new possibilities for enhancing the performance and reliability of GaN-based electronic devices through innovative dielectric materials and low-temperature deposition techniques.

The BN film deposition was performed by microwave-plasma-assisted chemical vapor deposition using ammonia borane as the precursor. A continuous flow of 20 sccm H_2 and 120 sccm N_2 gases was maintained throughout the growth to keep the pressure at around 1 Torr. When the AlGaN/GaN HEMT sample was heated to 400 °C, the microwave plasma was ignited and kept an output power at 1 kW. After 20 min growth, the microwave was switched off while the sample cooled down naturally. Following the BN deposition, surface analysis using X-ray photoelectron spectroscopy (XPS) was conducted to obtain chemical information. The XPS measurements were carried out using PHI Quantera SXM scanning X-ray microprobe with 1486.6 eV monochromatic Al Kα X-rays. Survey and high-resolution scans were recorded at 140 eV and 26 eV pass energy, respectively. The survey scan depicted in Figure 1(a) detected both B and N along with Al and Ga peaks originating from the HEMT sample. In the high-resolution XPS spectra presented in Figure

1(b) and 1(c), the binding energies of the B 1s and N 1s peaks were determined to be 190.7 eV and 398.2 eV, respectively, indicating the presence of sp2-bonded B and N in the films. Additionally, the B/N atomic ratio was determined to be 1.1:1. Reflection Electron Energy Loss Spectroscopy (REELS) spectra were collected by Nexsa G2 Surface Analysis System with an electron beam energy of 1 keV. REELS is a useful technique to measure band gaps of semiconductors and insulators, and the details of the technique can be found elsewhere.[43] It revealed a band gap of 5.79 eV for BN film (Figure 1(d)), which is consistent with previous reports.[12-14] Park Systems NX20 Atomic Force Microscope (AFM) was employed for surface topography imaging. The AFM measurements in Figure 1(d) and 1(e) disclosed a smooth surface for the BN film with a surface roughness of 1.3 nm. The results confirm the successful deposition of high-quality BN film on AlGaN/GaN HEMTs. The low surface roughness observed is beneficial for high-quality BN growth and minimizes etching on the AlGaN/GaN substrate, particularly at low deposition temperatures.

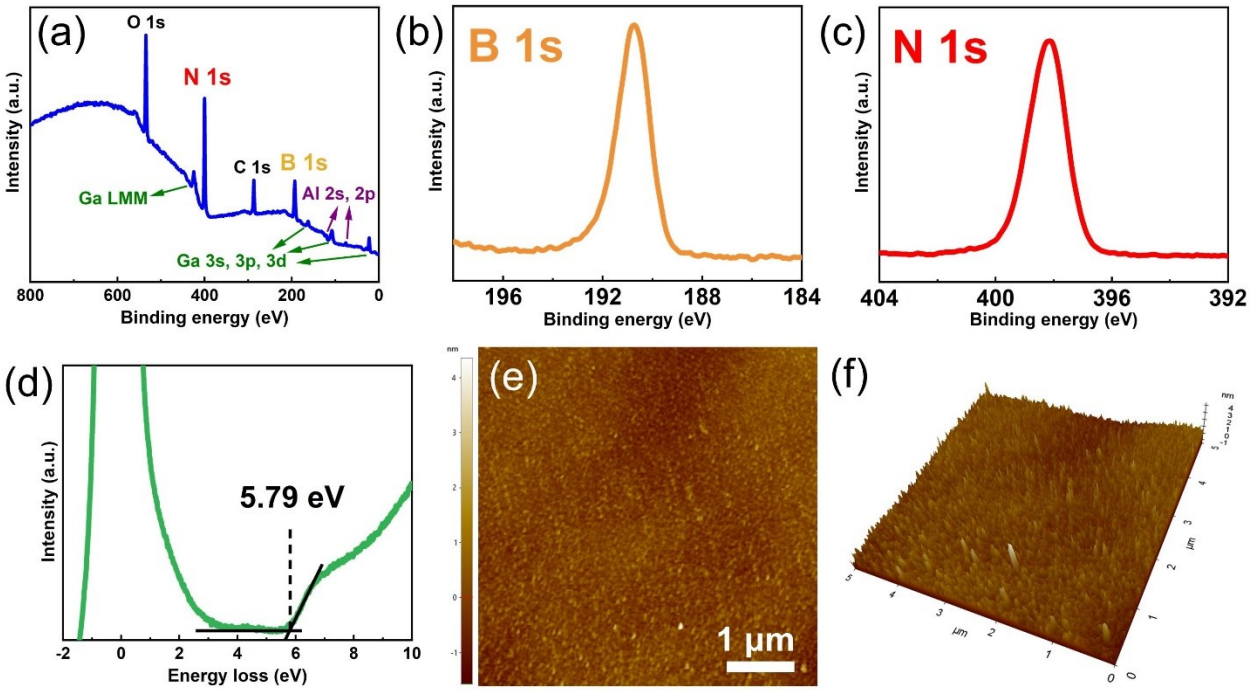

Figure 1. (a) XPS survey scan of BN on AlGaN/GaN. High-resolution elemental scans of (b) B 1s and (c) N 1s. (d) REELS spectra revealing the bandgap of BN film is 5.79 eV. (e) AFM 2D image and (f) 3D image of BN surface showing its exceptional smoothness

An optical image of a BN/AlGaN/GaN MISHEMT is presented in Figure 2(a). The drain, source, and gate electrodes are denoted as D, S, and G, respectively. Elemental depth profile analysis was conducted within the yellow dashed square using Time-of-Flight Secondary Ion Mass Spectrometry (ToF-SIMS). ToF-SIMS measurements were performed using a TOF-SIMS NCS instrument, which combines a TOF.SIMS5 instrument (ION-TOF GmbH, Münster, Germany) and an in-situ Scanning Probe Microscope (NanoScan, Switzerland) at Shared Equipment Authority

from Rice University. The analysis field of view was 90 x 90 μm^2 (Bi_3^+ @ 30keV, 0.2pA) with a raster of 256 by 256 along the 3D depth profile. A charge compensation with an electron flood gun has been applied during the analysis. An adjustment of the charge effects has been operated using a surface potential. The cycle times was fixed to 90 μs (corresponding to m/z = 0 – 911 a.m.u mass range). The sputtering raster was 450 x 450 μm^2 (Cs^+ @ 1keV, 85nA). The beams were operated in non-interlaced mode, alternating 1 analysis cycle and 1 frame of sputtering (corresponding to 1.64s) followed by a pause of 5s for the charge compensation.

Elemental mappings of B+, Ga+, and CsTi+ are depicted in Figure 2(b), 2(c), and 2(d), respectively. It is evident that B+ is concentrated at the center of the image, indicating the presence of the BN film. Ga+ is dispersed throughout the entire area, originating from the underlying AlGaN/GaN substrate. The slight non-uniformity observed near the edge of the gate electrodes may result from annealing during the fabrication process. CsTi+ is predominantly present in the left and right regions as only the drain and source electrodes contain Ti, not the gate electrode. All these element distributions align well with the device structure, affirming the success of the fabrication process. The cross-sectional specimen was prepared by using FEI Helios 660 FIB/SEM and imaged by FEI Titan Themis S/TEM. Cross-sectional transmission electron microscopy (TEM) images in Figure 2(e) illustrate the interface between BN and AlGaN/GaN, revealing a BN film thickness of approximately 11 nm. Furthermore, the BN film exhibits an amorphous nature without discernible long-range order, consistent with previous findings.[17,18] Figure 2(f) presents the high-angle annular dark-field (HAADF) image obtained at the interface between GaN and BN and the corresponding energy-dispersive X-ray (EDX) mappings of B and N. The HAADF image clearly demonstrates the atomic resolution of GaN lattice. According to the EDX mappings, B can be found only in the BN layer, while N disperses in the entire image, as both BN and GaN contain N. These results agree well with the interface structures. The electron energy loss spectroscopy (EELS) spectra (Figure 2(g)) extracted from the BN film distinctly demonstrated characteristic B and N K-shell peaks, along with a minor presence of amorphous carbon and oxygen.

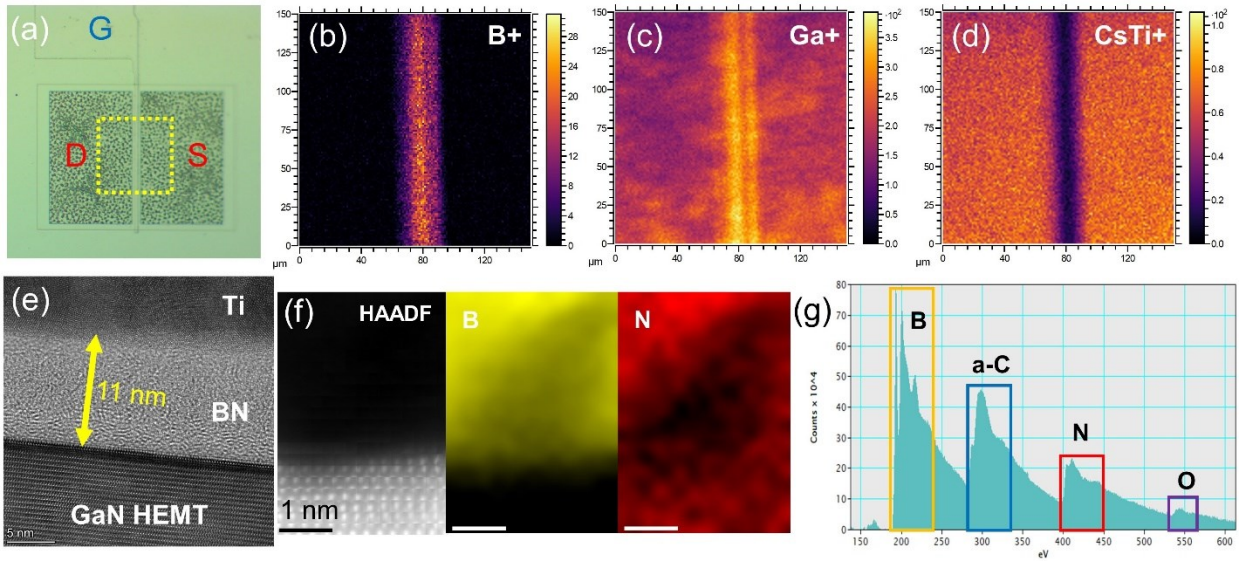

Figure 2. (a) Optical image of BN/AlGaN/GaN MISHEMT. G, D, and S are standard for gate, drain, and source electrodes. Elemental mapping of (b) B+, (c) Ga+, and (d) CsTi+ collected by ToF-SIMS. (e) Cross-sectional TEM image of BN on AlGaN/GaN. (f) HAADF image and corresponding EDX mapping of B and N. (g) EELS spectra of BN film.

The MISHEMT devices were fabricated on AlGaN/GaN epilayers grown by MOCVD on a p-type Si (111) substrate. The Al, Ga, and N sources are trimethylaluminum (TMAl), trimethylgallium (TMGa), and ammonia (NH_3), respectively. SiH_4 was used as an n-type dopant and H_2 was the carrier gas. The structure, from top to bottom, consisted of a 2.5 nm GaN cap layer, followed by a 20 nm $Al_{0.25}Ga_{0.75}N$ barrier layer, a 1 nm AlN interlayer, a 200 nm GaN layer, and a 4 µm GaN buffer layer on a silicon substrate. The cross-sectional schematic of the device structure is depicted in Figure 3(a), and Figure 3(b) shows a schematic of the fabrication process flow of the AlGaN/GaN MISHEMT after BN deposition. The mesa isolation was defined and etched by chlorine-based inductively coupled plasma-reactive ion etching (ICP-RIE). After mesa etching, the dielectric via hole for source and drain contacts was etched by SF_6-based ICP-RIE at low RF power, which selectively etches the BN at a rate of 36 nm/min without etching the GaN underneath. Afterward, Ti/Al/Ni/Au (25/100/15/50 nm) metal stack was deposited by electron beam evaporation followed by rapid thermal annealing at 850 °C for 30 s in N_2 ambient for ohmic contact formation. Finally, the Ni/Au (50/50 nm) gate metal stacks were deposited on the BN gate dielectric by electron beam evaporation. The MISHEMT devices had a gate width (W_G) of 100 µm, gate length (L_G) of 5 µm, gate-to-source distance (L_{GS}) of 4 µm, and gate-to-drain distance (L_{GD}) of 4 µm. The conventional Schottky-gate AlGaN/GaN HEMTs with the same geometry were also fabricated at the same time for reference.

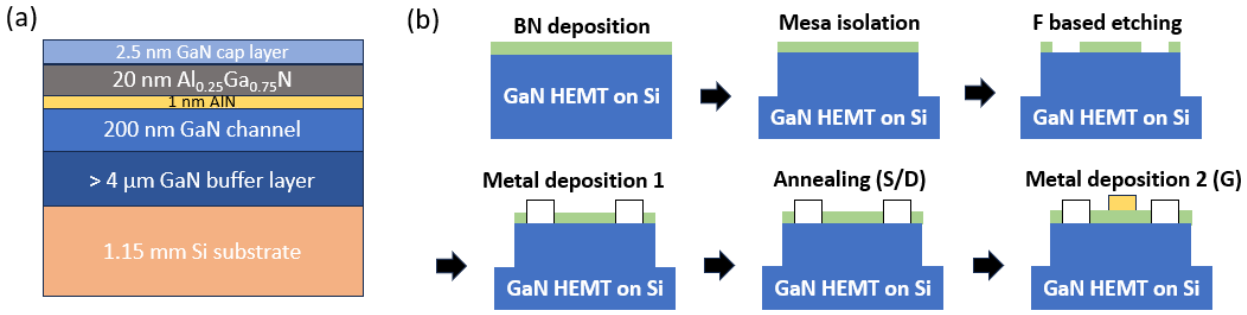

Figure 3. (a) Schematic of the AlGaN/GaN HEMT epilayer on Si substrate. (b) The fabrication process flow of the AlGaN/GaN MISHEMT after BN deposition.

Figure 4(a) shows the output characteristics of BN/AlGaN/GaN MISHEMTs and the conventional Schottky-gate AlGaN/GaN HEMTs. The V_{DS} was swept from 0 V to 10 V with V_{GS} between –3 V and 1 V with a step of 1 V. The BN MISHEMTs showed a higher maximum output current of 543 mA/mm compared to that of 433 mA/mm in Schottky-gate HEMT at V_{GS} = 1 V. And the on-resistance of the two devices was calculated to be 5.40 Ω·mm and 6.78 Ω·mm, respectively. The reduction of the on-resistance is likely related to reduced 2DEG resistance in the

MISHEMTs, which is possibly caused by the modification of the strain and piezoelectric polarization of the AlGaN barrier by the deposited gate dielectric.[19] Figure 4(b) shows the transfer characteristics of BN/AlGaN/GaN MISHEMTs and the Schottky-gate HEMT when V_{DS} = 1 V. The HEMTs had V_T of −3.2 V and $g_{m,\,max}$ of 62 mS/mm, while the MISHEMTs showed a threshold voltage of −5.9 V with a maximum transconductance $g_{m,\,max}$ of 42 mS/mm due to the BN insulator and the interface charge introduced. The MISHEMT devices exhibited a high I_{on}/I_{off} ratio of more than 10^8 compared with that of about 10^5 in Schottky gate HEMT, which is due to the effective suppression of reverse leakage current. The gate leakage–gate voltage (I_G–V_G) curves for the HEMT and MISHEMT are shown in Figure 4(c), where the drain voltage and source voltage were set as 0 V. A very low gate leakage current of ~10^{-7} mA/mm at reverse bias was observed in the MISHEMT, which is 3 orders of magnitude lower than the HEMT. This indicates the low-temperature CVD-grown BN gate dielectric is highly effective in suppressing gate leakage. Figure 4(d) shows the temperature-dependent I_G–V_G curve for the BN/AlGaN/GaN MISHEMT from 25 ℃ to 205 ℃, where the temperature dispersion of the leakage current the gate leakage is caused by thermal emission.[31]

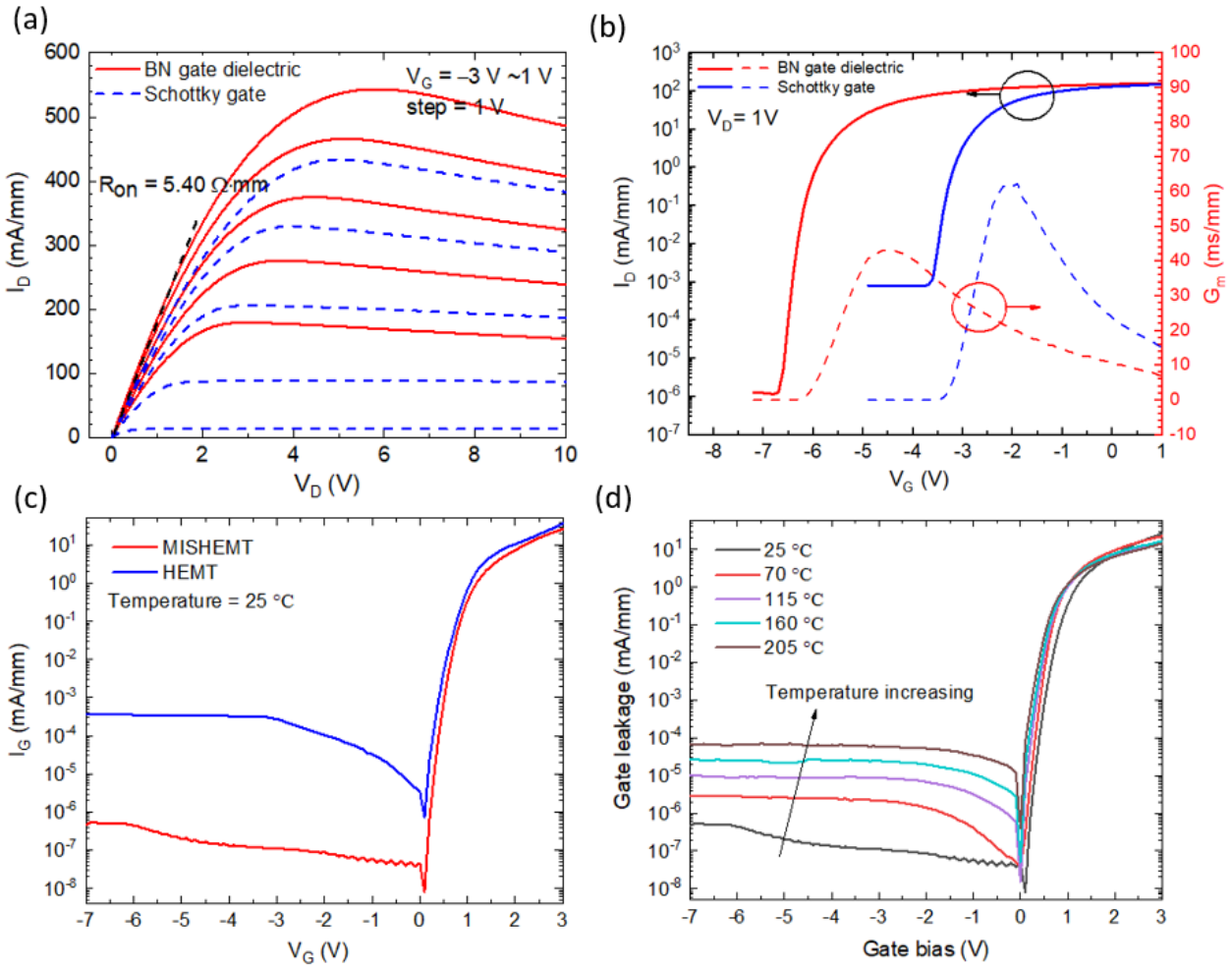

Figure 4. (a) I_D–V_D curves of the AlGaN/GaN HEMTs and BN/AlGaN/GaN MISHEMTs. (b) I_D–V_G curves of the AlGaN/GaN HEMTs and BN/AlGaN/GaN MISHEMTs. (c) I_G–V_G curves of

AlGaN/GaN HEMT and BN/AlGaN/GaN MISHEMTs at room temperature. (d) I_G–V_G curves of BN/AlGaN/GaN MISHEMT at the temperatures from 25 ℃ to 205 ℃.

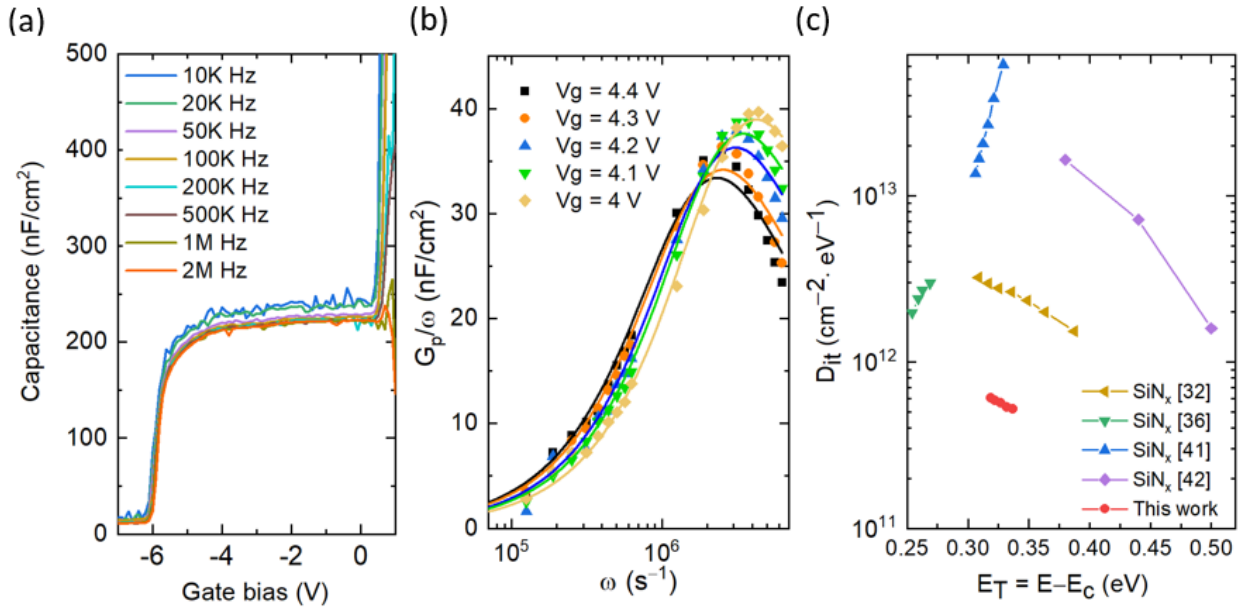

Figure 5. (a) The C-V curves of the BN/HEMT MIS diode at the frequencies from 10 kHz to 2 MHz. (b) G_p/ω versus ω of BN/HEMT MIS diodes at different gate biases. (c) Extracted D_{it} as a function of energy obtained by frequency-dependent conductance methods conducted at room temperature, and compared with the other results.

To gain more insights into the gate dielectric/HEMT interface quality, BN/HEMT MIS diode was also fabricated and characterized using capacitance-voltage (C-V) measurement. Figure 5(a) shows the frequency dispersion of between 10 kHz to 2 MHz for C-V curves of BN/HEMT MIS diodes. The frequency-dependent conductance measurement was performed at room temperature to determine the interface state traps (D_{it}) of the BN/HEMT interface.[32,36] Figure 5(b) shows the parallel conductance versus frequency data obtained for a MIS diode at different forward gate voltages, which corresponds to the barrier accumulation. While assuming a continuum of trap levels, the equivalent parallel conductance G_p as a function of frequency, can be expressed as[32]

$$\frac{G_p}{\omega} = \frac{qD_{it}}{2\omega\tau_{it}} \ln\left(1 + (\omega\tau_{it})^2\right)$$

where D_{it} is the trap density, τ_{it} is the trap state time constant, and ω is the radial frequency. The D_{it} and τ_{it} can be extracted by fitting the G_p/ω-ω plot as shown in Figure 5(b). The D_{it} at the certain trap energy level below the conduction band can be determined by using the time constant through the Shockley–Read–Hall statistics[32]

$$E_T = kTln(\tau_T N_c v_t \sigma_T)$$

where N_c=4.3×10^{14}×T$^{3/2}$ cm^{-3} is the effective density of states in the conduction band in the semiconductor, v_t=2×10^7 cm·s^{-1} is the average thermal velocity of electrons, and σ_T=1×10^{-14} cm^2

is the capture cross-section of the trap states.[32] The D_{it} as a function of their energy (E_T) for the MIS diodes is shown in Figure 5(c), and compared with the other works. Remarkably, a low interface trap state density of 5.2×10^{11} $cm^{-2}\cdot eV^{-1}$ to 6.1×10^{11} $cm^{-2}\cdot eV^{-1}$ at the trap energy from 0.34 eV to 0.32 eV was obtained, which is notably lower than typical CVD and ALD deposited dielectrics.[32-42] These results signify the high quality of the BN/HEMT interface established in this work. Table 1 shows the comparison of reported AlGaN/GaN MISHEMTs with different CVD-grown dielectrics. With the lowest CVD growth temperature, this work exhibits a very low dielectric/nitride interface charge density, and a low reverse leakage current for AlGaN/GaN MISHEMTs. The leakage current and interface charge density could be further reduced if the higher growth temperature is adopted.[1]

Table 1. The comparison of this work and other reported MISHEMTs with different dielectrics

Gate dielectric	Growth temperature (°C)	Reverse gate leakage (mA/mm)	Interface charge density ($cm^{-2}\cdot eV^{-1}$)
BN (This work)	400	5×10^{-7}	5.2×10^{11}-6.1×10^{11}
BN [10]	825	10^{-8}	$< 8.49\times10^{11}$
SiN_x [36]	1125	2×10^{-6}	$\sim3\times10^{12}$
SiN_x [41]	780	10^{-8}	1.4×10^{13}-5.3×10^{13}
SiN_x [42]	650	2×10^{-7}	2.6×10^{13}

In summary, high-quality low-temperature CVD-grown BN was used as gate dielectric for AlGaN/GaN MISHEMT with significant performance improvements compared with conventional Schottky-gate HEMT. Comprehensive material characterizations were performed on the BN film, including XPS, REELS, AFM, ToF-SIMS, and HRTEM. The MISHEMT devices exhibited a high on/off current ratio of 10^8, a threshold voltage of −5.9 V, a low reverse gate leakage current of 5×10^{-7} mA/mm, and a high maximum transconductance of 42 mS/mm. Notably, compared with the conventional HEMTs, BN/AlGaN/GaN MISHEMTs showed a significant reduction of reverse gate leakage by three orders of magnitude and a higher output current. A low D_{it} in the range of 5.2×10^{11} to 6.1×10^{11} $cm^{-2}\cdot eV^{-1}$ obtained by frequency-dependent conductance methods suggests a good interface quality between BN and HEMT surface. These results provide valuable insights for the future development of high-performance GaN MISHEMT for power and RF electronics.

AUTHOR DECLARATIONS

Conflict of Interest

The authors have no conflicts to disclose.

ACKNOWLEDGMENTS

This work is supported as part of ULTRA, an Energy Frontier Research Center funded by the U.S. Department of Energy, Office of Science, Basic Energy Sciences under Award No. DE-SC0021230. This work is also supported by the National Science Foundation (NSF) under Award No. ECCS-2302696 and No. ECCS-2338604. This work is in part supported by Applied Materials. This work is also supported by CHIMES, one of the Seven Centers in JUMP 2.0, a Semiconductor Research Corporation (SRC) Program by DARPA. This work uses ASU NanoFab Facilities, supported in part by the National Science Foundation under Award No. ECCS-2025490. ToF-SIMS analysis was carried out with support provided by the National Science Foundation CBET-1626418. This work was conducted in part using resources of the Shared Equipment Authority at Rice University.

DATA AVAILABILITY

The data that support the findings of this study are available from the corresponding author upon reasonable request.

REFERENCES

[1] H. Amano, Y. Baines, E. Beam, M. Borga, T. Bouchet, P. R. Chalker, M. Charles, K. J. Chen, N. Chowdhury, R. Chu, C. De Santi, M. M. De Souza, S. Decoutere, L. Di Cioccio, B. Eckardt, T. Egawa, P. Fay, J. J. Freedsman, L. Guido, O. Häberlen, G. Haynes, T. Heckel, D. Hemakumara, P. Houston, J. Hu, M. Hua, Q. Huang, A. Huang, S. Jiang, H. Kawai, D. Kinzer, M. Kuball, A. Kumar, K. B. Lee, X. Li, D. Marcon, M. März, R. McCarthy, G. Meneghesso, M. Meneghini, E. Morvan, A. Nakajima, E. M. S. Narayanan, S. Oliver, T. Palacios, D. Piedra, M. Plissonnier, R. Reddy, M. Sun, I. Thayne, A. Torres, N. Trivellin, V. Unni, M. J. Uren, M. Van Hove, D. J. Wallis, J. Wang, J. Xie, S. Yagi, S. Yang, C. Youtsey, R. Yu, E. Zanoni, S. Zeltner, and Y. Zhang, "The 2018 GaN power electronics roadmap," J. Phys. D 51(16), 163001 (2018)

[2] J. Q. He, W. C. Cheng, Q. Wang, K. Cheng, H. Y. Yu, and Y. Chai, "Recent Advances in GaN-Based Power HEMT Devices," Adv. Electron. Mater. 7, 2001045 (2021).

[3] T. Hashizume, K. Nishiguchi, S. Kaneki, J. Kuzmik, and Z. Yatabe, "State of the art on gate insulation and surface passivation for GaN-based power HEMTs," Mat. Sci. Semicond. Proc. 78, 85 (2018).

[4] J. Y. Tsao, S. Chowdhury, M. A. Hollis, D. Jena, N. M. Johnson, K. A. Jones, R. J. Kaplar, S.

Rajan, C. G. Van de Walle, E. Bellotti, C. L. Chua, R. Collazo, M. E. Coltrin, J. A. Cooper, K. R. Evans, S. Graham, T. A. Grotjohn, E. R. Heller, M. Higashiwaki, M. S. Islam, P. W. Juodawlkis, M. A. Khan, A. D. Koehler, J. H. Leach, U. K. Mishra, R. J. Nemanich, R. C. N. Pilawa-Podgurski, J. B. Shealy, Z. Sitar, M. J. Tadjer, A. F. Witulski, M. Wraback, and J. A. Simmons, "Ultrawide-bandgap semiconductors: Research opportunities and challenges," Advanced Electronic Materials 4 (1) (2017).

[5] M. Xu, D. Wang, K. Fu, D. H. Mudiyanselage, H. Fu, and Y. Zhao, "A review of ultrawide bandgap materials: Properties, synthesis and devices," Oxford Open Mater. Sci. 2, itac004 (2022).

[6] S. Roy, X. Zhang, A.B. Puthirath, A. Meiyazhagan, S. Bhattacharyya, M.M. Rahman, G. Babu, S. Susarla, S.K. Saju, M.K. Tran, L.M. Sassi, M.A.S.R. Saadi, J. Lai, O. Sahin, S.M. Sajadi, B. Dharmarajan, D. Salpekar, N. Chakingal, A. Baburaj, X. Shuai, A. Adumbumkulath, K.A. Miller, J.M. Gayle, A. Ajnsztajn, T. Prasankumar, V.V.J. Harikrishnan, V. Ojha, H. Kannan, A.Z. Khater, Z. Zhu, S.A. Iyengar, P.A. da S. Autreto, E.F. Oliveira, G. Gao, A.G. Birdwell, M.R. Neupane, T.G. Ivanov, J. Taha-Tijerina, R.M. Yadav, S. Arepalli, R. Vajtai, and P.M. Ajayan, "Structure, Properties and Applications of Two-Dimensional Hexagonal Boron Nitride," Adv. Mater. 33(44), 2101589 (2021).

[7] Z. He, K. Fu, M. Xu, J. Zhou, T. Li, and Y. Zhao, "Understanding the Breakdown Behavior of Ultrawide-Bandgap Boron Nitride Power Diodes Using Device Modeling," Phys. Status Solidi RRL 2200397 (2021).

[8] A. Biswas, M. Xu, K. Fu, J. Zhou, R. Xu, A.B. Puthirath, J.A. Hachtel, C. Li, S.A. Iyengar, H. Kannan, X. Zhang, T. Gray, R. Vajtai, A. Glen Birdwell, M.R. Neupane, D.A. Ruzmetov, P.B. Shah, T. Ivanov, H. Zhu, Y. Zhao, and P.M. Ajayan, "Properties and device performance of BN thin films grown on GaN by pulsed laser deposition," Appl. Phys. Lett. 121(9), 92105 (2022).

[9] B. Ren, M. Liao, M. Sumiya, J. Li, L. Wang, X. Liu, Y. Koide, and L. Sang, "Layered boron nitride enabling high-performance AlGaN/GaN high electron mobility transistor," J. Alloys Compd. 829, 154542 (2020).

[10] T.H. Yang, J. Brown, K. Fu, J. Zhou, K. Hatch, C. Yang, J. Montes, X. Qi, H. Fu, R.J. Nemanich, and Y. Zhao, "AlGaN/GaN metal-insulator-semiconductor high electron mobility transistors (MISHEMTs) using plasma deposited BN as gate dielectric," Appl. Phys. Lett. 118(7), (2021).

[11] S. Moon, S.J. Chang, Y. Kim, O.F.N. Okello, J. Kim, J. Kim, H.W. Jung, H.K. Ahn, D.S. Kim, S.Y. Choi, J. Lee, J.W. Lim, and J.K. Kim, "Van der Waals Heterostructure of Hexagonal Boron Nitride with an AlGaN/GaN Epitaxial Wafer for High-Performance Radio Frequency Applications," ACS Appl. Mater. Interfaces 13(49), 59440–59449 (2021).

[12] M. Yamamoto, H. Murata, N. Miyata, H. Takashima, M. Nagao, H. Mimura, Y. Neo, and K. Murakami, "Low-Temperature Direct Synthesis of Multilayered h-BN without Catalysts by Inductively Coupled Plasma-Enhanced Chemical Vapor Deposition," ACS Omega 8(6), 5497–5505 (2023).

[13] K. Watanabe, T. Taniguchi, and H. Kanda, "Direct-bandgap properties and evidence for ultraviolet lasing of hexagonal boron nitride single crystal," Nat. Mater. 2004 36 3(6), 404–409 (2004).

[14] K. Yi, Z. Jin, S. Bu, D. Wang, D. Liu, Y. Huang, Y. Dong, Q. Yuan, Y. Liu, A.T.S. Wee, and

D. Wei, “Catalyst-Free Growth of Two-Dimensional BCxN Materials on Dielectrics by Temperature-Dependent Plasma-Enhanced Chemical Vapor Deposition,” ACS Appl. Mater. Interfaces 12(29), 33113–33120 (2020).

[15] G. H. Lee, A.H. Park, J.H. Lim, C.-H. Lee, D.-W. Jeon, Y.-B. Kim, J. Lee, J.W. Yang, E.-K. Suh, and T.H. Seo, “Boron Nitride as a Passivation Capping Layer for AlGaN/GaN High Electron Mobility Transistors,” J. Nanosci. Nanotechnol. 20(7), 4450–4453 (2020).

[16] E. Zdanowicz, A.P. Herman, K. Opołczyńska, S. Gorantla, W. Olszewski, J. Serafińczuk, D. Hommel, and R. Kudrawiec, “Toward h-BN/GaN Schottky Diodes: Spectroscopic Study on the Electronic Phenomena at the Interface,” ACS Appl. Mater. Interfaces 14(4), 6131–6137 (2022).

[17] S. Hong, C.S. Lee, M.H. Lee, Y. Lee, K.Y. Ma, G. Kim, S.I. Yoon, K. Ihm, K.J. Kim, T.J. Shin, S.W. Kim, E. chae Jeon, H. Jeon, J.Y. Kim, H.I. Lee, Z. Lee, A. Antidormi, S. Roche, M. Chhowalla, H.J. Shin, and H.S. Shin, “Ultralow-dielectric-constant amorphous boron nitride,” Nature 582(7813), 511–514 (2020).

[18] D. Liu, X. Chen, Y. Yan, Z. Zhang, Z. Jin, K. Yi, C. Zhang, Y. Zheng, Y. Wang, J. Yang, X. Xu, J. Chen, Y. Lu, D. Wei, A.T.S. Wee, and D. Wei, “Conformal hexagonal-boron nitride dielectric interface for tungsten diselenide devices with improved mobility and thermal dissipation,” Nat. Commun. 10(1), (2019).

[19] M. Y. Hua, C. Liu, S. Yang, S. H. Liu, K. Fu, Z. H. Dong, Y. Cai, B. S. Zhang, and K. J. Chen, “Characterization of Leakage and Reliability of SiNx Gate Dielectric by Low-Pressure Chemical Vapor Deposition for GaN-based MIS-HEMTs,” IEEE Trans. Electron Devices 62, 3215 (2015).

[20] S. S. Chng, M. Zhu, Z. Du, X. Wang, M. Whiteside, Z. K. Ng, M. Shakerzadeh, S. H. Tsang, E. H. T. Teo, “Dielectric dispersion and superior thermal characteristics in isotope-enriched hexagonal boron nitride thin films: evaluation as thermally self-dissipating dielectrics for GaN transistor,” J. Mater. Chem. C 8, 9558 (2020).

[21] J.-C. Gerbedoen, A. Soltani, M. Mattalah, M. Moreau, P. Thevenin, and J.-C. De Jaeger, “AlGaN/GaN MISHEMT with hBN as gate dielectric,” Diamond Relat. Mater. 18(5-8), 1039 (2009).

[22] J. Vanjaria, A. C. Arjunan, Y. Wu, G. S. Tompa, H. Yu, “Epitaxial Ge thin film Growth on Si Using a Cost-Effective Process in Simplified CVD Reactor,” ECS J. Solid State Sci. Technol. 9, 034008 (2020).

[23] M. Whiteside, S. Arulkumaran, and G. I. Ng, “Demonstration of vertically-ordered h-BN/AlGaN/GaN metal-insulator-semiconductor high-electron-mobility transistors on Si substrate,” Mater. Sci. Eng. B 270, 115224 (2021).

[24] M. Xu, A. Biswas, T. Li, Z. He, S. Luo, Z. Mei, J. Zhou, C. Chang, A. B. Puthirath, R. Vajtai, P. M. Ajayan, and Y. Zhao, “Vertical β-Ga2O3 metal–insulator–semiconductor diodes with an ultrathin boron nitride interlayer,” Appl. Phys. Lett. 123, 232107 (2023).

[25] G. Ye, H. Wang, S. Arulkumaran, G. I. Ng, R. Hofstetter, Y. Li, M. J. Anand, K. S. Ang, Y. K. T. Maung, and S. C. Foo, “Atomic layer deposition of ZrO2 as gate dielectrics for AlGaN/GaN metal-insulator-semiconductor high electron mobility transistors on silicon,” Appl. Phys. Lett. 103, 142109 (2013).

[26] Y. Wu, and H. Yu, “A Low-Cost Novel Method to Fabricate Integrated Magnetic Core Inductor Embedded in Organic Substrate,” IEEE Trans. Magn. 58, 8 (2022).

[27] Y. Wu, I.-C. Yeng and H. Yu, “The improvement of CoZrTaB thin films on different substrates for flexible device applications,” AIP Adv. 11, 2 (2021).

[28] K. Fu, S. Luo, H. Fu, K. Hatch, S. R. Alugubelli, H. Liu, T. Li, M. Xu, Z. Mei, Z. He, J. Zhou, C. Chang, F. A. Ponce, R. Nemanich, and Y. Zhao, “GaN-based threshold switching behaviors at high temperatures enabled by interface engineering for harsh environment memory applications,” IEEE Trans. Electron Devices 1, 1–5 (2023)

[29] J. Vanjaria, V. Hariharan, A. C. Arjunan, Y. Wu, G. S. Tompa, and H. Yu, "One-Step Cost-Effective Growth of High-Quality Epitaxial Ge Films on Si (100) Using a Simplified PECVD Reactor." Electron. Mater. 2, 482 (2021).

[30] S. Grenadier, J. Li, J. Lin, and H. Jiang, “Dry etching techniques for active devices based on hexagonal boron nitride epilayers,” J. Vac. Sci. Technol. A 31(6), 061517 (2013).

[31]W. Lim, J.-H. Jeong, J.-H. Lee, S.-B. Hur, J.-K. Ryu, K.-S. Kim, T.-H. Kim, S. Y. Song, J.-I. Yang, and S. J. Pearton, “Temperature dependence of current-voltage characteristics of Ni–AlGaN/GaN Schottky diodes,” Appl. Phys. Lett. 97 (24) (2010).

[32] X. Lu, J. Ma, H. Jiang, C. Liu, and K. M. Lau, “Characterization of in situ SiNx thin film grown on AlN/GaN heterostructure by metalorganic chemical vapor deposition,” Appl. Phys. Lett. 105, 102911 (2014).

[33] S. Liu, S. Yang, Z. Tang, Q. Jiang, C. Liu, M. Wang, and K. J. Chen, “Al2O3/AlN/GaN MOS-Channel-HEMTs With an AlN Interfacial Layer,” IEEE Electron Device Lett. 35, 723 (2014).

[34] P. Kordoš, R. Stoklas, D. Gregušová, and J. Novák, “Characterization of AlGaN/GaN metal-oxide-semiconductor field-effect transistors by frequency dependent conductance analysis,” Appl. Phys. Lett. 94, 223512 (2009).

[35] M. Hua, C. Liu, S. Yang, S. Liu, K. Fu, Z. Dong, Y. Cai, B. Zhang, and K. J. Chen, “GaN-Based Metal-Insulator-Semiconductor High-Electron-Mobility Transistors Using Low-Pressure Chemical Vapor Deposition SiNx as Gate Dielectric,” IEEE Electron Device Lett. 36, 448 (2015).

[36] H. X. Jiang, C. Liu, Y. Y. Chen, X. Lu, C. W. Tang, and K. M. Lau, “Investigation of In Situ SiN as Gate Dielectric and Surface Passivation for GaN MISHEMT,” IEEE Trans. Electron Devices 64, 832 (2017).

[37] J.-J. Zhu, X.-H. Ma, Y. Xie, B. Hou, W.-W. Chen, J.-C. Zhang, and Y. Hao, “Improved interface and transport properties of AlGaN/GaN MIS-HEMTs with PEALD-grown AlN gate dielectric,” IEEE Trans. Electron Devices 62, 512 (2015).

[38] H. Kim, H. J. Yun, S. Choi, and B. J. Choi, “Interface trap characterization of AlN/GaN heterostructure with Al2O3, HfO2, and HfO2/Al2O3 dielectrics,” J. Vac. Sci. Technol. B 37, 041203 (2019).

[39] S. Liu, S. Yang, Z. Tang, Q. Jiang, C. Liu, M. Wang, B. Shen, and K. J. Chen, “Interface/border trap characterization of Al2O3/AlN/GaN metal-oxide-semiconductor structures with an AlN interfacial layer,” Appl. Phys. Lett. 106, 051605 (2015).

[40] S. Yang, Z. Tang, K.-Y. Wong, Y.-S. Lin, C. Liu, Y. Lu, S. Huang, and K. J. Chen, "High-Quality Interface in Al2O3/GaN/AlGaN/GaN MIS Structures With In Situ Pre-Gate Plasma Nitridation," IEEE Electron Device Lett. 34, 1497 (2013).

[41] Z. Zhang, G. Yu, X. Zhang, X. Deng, S. Li, Y. Fan, S. Sun, L. Song, S. Tan, and D. Wu, "Studies on High-Voltage GaN-on-Si MIS-HEMTs Using LPCVD Si3N4 as Gate Dielectric and Passivation Layer," IEEE Trans. Electron Devices 63(2), 731 (2016).

[42] Z. Liu, S. Huang, Q. Bao, X. Wang, K. Wei, H. Jiang, H. Cui, J. Li, C. Zhao, X. Liu, J. Zhang, Q. Zhou, W. Chen, B. Zhang, and L. Jia, "Investigation of the interface between LPCVD-SiNx gate dielectric and III-nitride for AlGaN/GaN MIS-HEMTs," J. Vac. Sci. Technol., B: Nanotechnol. Microelectron.: Mater., Process., Meas., Phenom. 34 (4) (2016).

[43] M. Vos, S. W. King, B. L. French, "Measurement of the band gap by reflection electron energy loss spectroscopy," J. Electron Spectrosc. Relat. Phenom. 212, 74 (2016).